

## FAST TRACK COMMUNICATION

# Enhanced ferromagnetic Fe-rich germanide film grown using magnetron sputtering employing a post-deposition anneal

Andrew S W Wong<sup>1,3</sup>, Ghim W Ho<sup>2</sup> and Dong Z Chi<sup>1,3</sup><sup>1</sup>Institute of Materials Research and Engineering, A\*STAR (Agency for Science Technology and Research), 3 Research Link, Singapore 117602, Singapore<sup>2</sup>Engineering Science Programme, Department of Electrical and Computer Engineering, National University of Singapore, 5 Engineering Drive 2, Singapore 117576, SingaporeE-mail: [wonga@imre.a-star.edu.sg](mailto:wonga@imre.a-star.edu.sg) and [dz-chi@imre.a-star.edu.sg](mailto:dz-chi@imre.a-star.edu.sg)

Received 19 November 2007, in final form 28 December 2007

Published 1 February 2008

Online at [stacks.iop.org/JPhysD/41/042004](http://stacks.iop.org/JPhysD/41/042004)**Abstract**

We describe the formation of a ferromagnetic Fe-rich germanide layer by a two-step process involving magnetron sputtering and annealing. A thin epitaxial iron (epi-Fe) film is deposited on the Ge (001) substrate and then annealed at 275 °C in nitrogen inducing germanide formation. Surprisingly, we observe an enhancement in saturation magnetization in germanide films. Secondary ion mass spectroscopy and x-ray diffraction confirm the formation of a thin Fe-rich germanide layer whilst high resolution transmission electron imaging suggests it to be Fe<sub>3</sub>Ge.

(Some figures in this article are in colour only in the electronic version)

**1. Introduction**

The successful integration of ferromagnetic thin films onto semiconducting substrates provides an exciting route to exploration and exploitation of these devices for numerous applications, in particular spintronics [1]. Ferromagnetic metals on semiconductor surfaces can allow the injection of spin-polarized electrons into the semiconductor [2]. In particular, Fe films have been successfully grown on GaAs substrates using molecular beam epitaxy (MBE) and ion-beam sputtering due to the small (~1.4%) lattice mismatch between film and substrate [3–7]. Fe can also be grown on Ge using MBE due to the small mismatch of ca 1.3% between 2 unit cells of bcc-Fe (2.867 Å) and 1 unit cell of the Ge lattice ( $a_0 = 5.658$  Å) [8,9]. Very recently, Lou *et al* [10] demonstrated epitaxial growth of Fe on the Ge (001) substrates using magnetron sputtering above room temperature. One commonly cited problem for Fe

deposition on Ge surfaces is severe intermixing [11] between the Fe and Ge atoms at elevated temperatures. Intermixing can form 10 nm thick amorphous and/or crystalline Fe–Ge alloys which are reported to be magnetically dead [8, 11]. This phenomenon inevitably limits the deposition temperature of epi-Fe on Ge to between 100 and 150 °C [10] and also the temperature at which the device can operate.

In this paper, we report the formation of a Fe-rich germanide layer by magnetron sputtering, by employing a short nitrogen anneal at 275 °C to induce germanidation. We used bright field transmission electron microscopy (BFTEM) to observe the reaction between the Fe film and Ge substrate. High-resolution transmission electron microscopy (HRTEM) allows us to study the structure of the germanide layer. Furthermore, by using field-dependent magnetization loops, we demonstrate the enhancement in saturation magnetization of the epi-Fe compared with polycrystalline Fe (poly-Fe) films. Our study shed new light into the understanding of intermixing on the ferromagnetic property of Fe.

<sup>3</sup> Authors to whom any correspondence should be addressed.

## 2. Experimental methods

Standard substrate cleaning using acetone, ethanol and dilute hydrofluoric acid was carried out on all the Ge (001) substrates used in this work. The Ge substrates were immediately loaded into the sputtering chamber after cleaning. Magnetron sputtering was carried out in a Denton vacuum sputtering system. A 3 in. Fe target of 99.99% purity was used. Fe of 20–30 nm was deposited on Ge using Ar gas at sputtering rate of  $0.35 \text{ \AA s}^{-1}$ . Chamber base and working pressures were kept at  $5 \times 10^{-7}$  Torr and  $2.5 \times 10^{-3}$  Torr, respectively. The Ar gas flow rate was maintained at 25 sccm. Epi-Fe films were deposited at a substrate temperature of 180 °C. A set of control samples was deposited at room temperature ( $\sim 20$  °C). Rapid thermal annealing (RTA) was carried out in nitrogen at 275 °C and 475 °C for 60 s.

X-ray diffraction (XRD) analysis was carried out with Cu  $K_{\alpha}$  x-rays using a PANalytical X'Pert PRO XRD system operated at 40 kV and 40 mA. The Ge (004) peak was used for calibration of diffraction peak positions. The Ge (004) peak and peaks close to the substrate peak can be detected using this system. In addition, a general area detector diffraction system (GADDS) which has greater sensitivity than the PANalytical X'pert PRO system has also been employed to scan for polycrystalline peaks. Special care was taken to avoid the intense Ge (004) substrate peak to prevent saturation of the x-ray detector. The Cu  $K_{\alpha}$  x-rays were generated with 40 kV and 40 mA. The GADDS results are not presented in this paper.

The Fe samples were studied using time-of-flight secondary ion mass spectroscopy (TOF-SIMS). For SIMS analysis, an area of  $200 \mu\text{m} \times 200 \mu\text{m}$  was sputtered with 1 keV  $\text{Ar}^+$  ions. An area of  $100 \mu\text{m} \times 100 \mu\text{m}$  was analysed with 25 keV  $\text{Ga}^+$  ions. The  $^{74}\text{Ge}$  profile was used instead of the  $^{54}\text{Fe}$  profile to determine the interface due to the ion 'knock-in' effect of SIMS.

Cross-sectional TEM samples were prepared using conventional mechanical grinding and polishing techniques. This was followed by mechanical dimpling using a Gatan dimpling system. Electron transparent regions were formed by  $\text{Ar}^+$  milling using a Gatan precision ion polishing system at 5 keV (gun angles 8°) initially and 3 keV (gun angles 4°) when a hole was formed. The latter step was employed to minimize the extent of sample damage due to  $\text{Ar}^+$  milling at 5 keV. Normal bright field and high resolution transmission electron imaging were carried out in a Phillips CM300 high resolution transmission electron microscope, equipped with a field emission source operated at 300 kV. Energy dispersive x-ray spectroscopy (EDX) was carried out in a JEOL 2100 TEM in the scanning electron transmission electron (STEM) mode, operated at 200 kV.

Field-dependent magnetization loops were measured in-plane using an ADE Technologies Model 886 vibration sample magnetometer. Measurements were performed at room temperature.

## 3. Results and discussion

Figure 1 shows the x-ray patterns taken from poly-Fe and epi-Fe films. A  $2\theta$  peak at  $44.7^\circ$  attributed to the Fe (110) can

be observed for the poly-Fe film. This is consistent with the 2-dimensional (2D) Debye ring corresponding to the (110)-oriented Fe obtained from the GADDS (not presented here). For the Fe films deposited at 180 °C, a non-substrate peak at  $2\theta = 65.16^\circ$  attributed to bcc Fe (200) can be observed. This suggests that the Fe (001) are parallel to the Ge (001) planes, evidence of epitaxial growth of Fe on Ge. The Ge (004) peak is observed at  $66.01^\circ$  in all samples. No other peaks are observed at  $2\theta$  values between  $43^\circ$  and  $67^\circ$ . The GADDS result also show the absence of the polycrystalline bcc Fe (110) ring. Cross-sectional HRTEM images (figure 1(b)) taken along the Ge  $\langle 110 \rangle$  zone axis clearly show the polycrystalline nature of the Fe film deposited at room temperature. Inset I shows a selected area electron diffraction (SAED) pattern taken from a region including the Ge substrate and poly-Fe film. The sharp diffraction spots can be attributed to the single crystal Ge substrate whilst the low intensity diffraction ring is attributed to the Fe (110). Figure 1(c) shows the (110) planes of the epi-Fe film, perpendicular to the atomically sharp interface. No diffraction contrast or lattice fringes due to Fe–Ge alloy layers can be observed. Insets II and III show convergent beam electron diffraction (CBED) patterns for the epi-Fe film and Ge substrate, which shows the single crystal nature of both the Fe film and Ge substrate. The orientation relationship between the Fe film and Ge substrate is determined to be  $\langle 110 \rangle \text{ Fe} \parallel \langle 110 \rangle \text{ Ge}$  and  $\{002\} \text{ Fe} \parallel \{002\} \text{ Ge}$ , which consistent with the epitaxial growth of Fe on Ge (001). Secondary ion mass spectroscopy used to study intermixing of the Fe and Ge upon annealing shows interdiffusion of Ge at 275 °C and complete Fe intermixing at 475 °C for both poly- and epi-Fe films. XRD results (not presented here) confirm the formation of FeGe (iron mono-germanide) from poly-Fe at 475 °C. By using the Fe/Ge intensity ratio as a standard for 50 at % Fe and 50 at % Ge in the FeGe phase, and comparing this with the Fe/Ge intensity ratio of the thin layers formed at 275 °C, we can unambiguously conclude that the layers formed at 275 °C are Fe-rich germanides.

BFTEM was used to determine the thickness of the as-deposited and annealed films. The TEM specimens were tilted to edge-on condition for accurate assessment of the film thickness. The results are shown in table 1. The numbers in brackets indicates the percentage increase in thickness or volume after anneal. The thickness increased after a nitrogen anneal at 275 °C by ca 6 nm and ca 3 nm for the poly-Fe RTA and epi-Fe film, respectively. We suggest that the larger thickness change (or volume expansion) in the poly-Fe film at 275 °C is due to a stronger intermixing between Fe and Ge in the polycrystalline Fe. At 475 °C, the thickness increased by ca 30 nm and ca 21.5 nm, which can be translated to  $\sim 100\%$  increase in volume (table 1), for poly- and epi-Fe films, respectively. The total thickness of the germanide film depends on the initial thickness of the as-deposited films. Inspection of the epi-Fe film/Ge substrate interface annealed at 275 °C (figure 2(a)) shows a band of dark contrast ca 7 nm thick. Within this band (figure 2(a)) the Fe (110) planes perpendicular to the interface can still be observed. This can be attributed to Fe and Ge intermixing but which did not significantly disrupt the epi-Fe lattice. The dark band

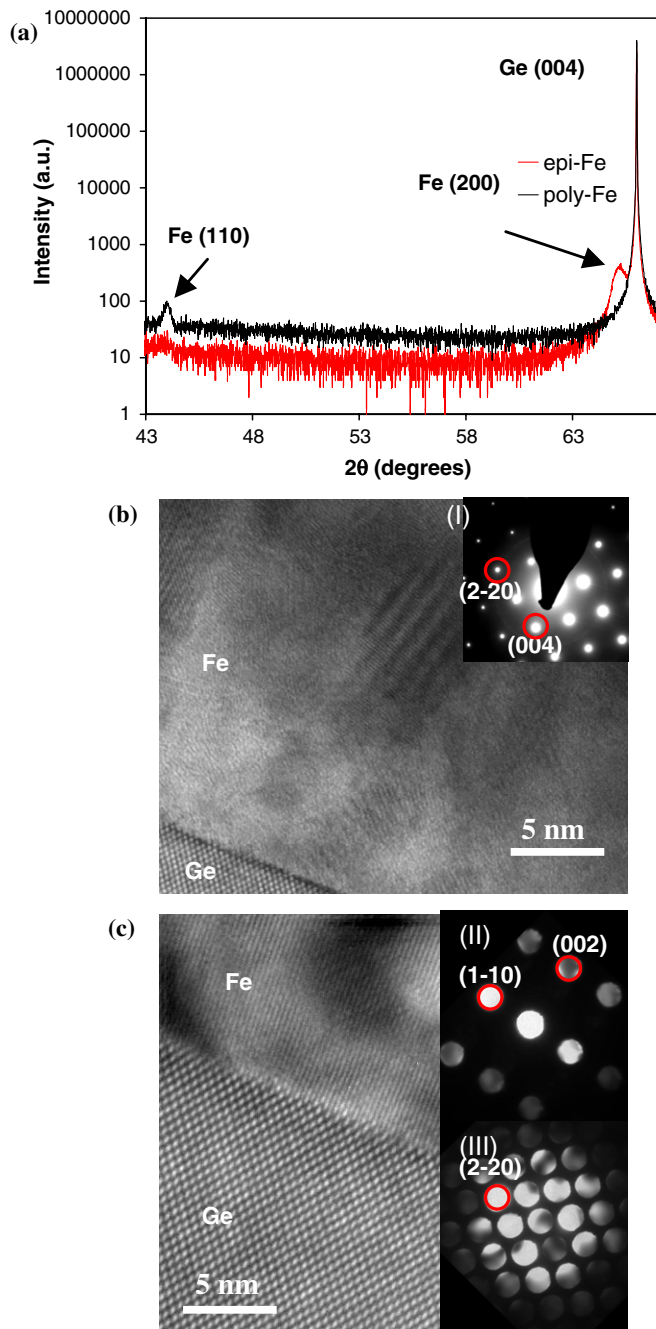


**Figure 1.** (a) XRD patterns of poly- and epi-Fe films deposited on Ge (001) substrates. (b) HRTEM images of poly-Fe film taken down the  $\langle 110 \rangle$  zone axis; inset I shows the SAED pattern with the polycrystalline Fe  $\langle 110 \rangle$  ring clearly visible. (c) HRTEM image taken down the  $\langle 110 \rangle$  zone axis, showing the Fe  $\langle 110 \rangle$  perpendicular to the interface. Insets (II) and (III) are the CBED patterns taken from the epi-Fe and Ge substrate, respectively. Circles highlight the spots with corresponding crystallographic indices.

can be caused by compositional and diffraction contrast. Ge atoms scatter electron more strongly than Fe atoms due to the larger atomic mass of the former. This phenomenon results in compositional contrast and the germanide layer will appear darker than the un-reacted epi-Fe. However, the thin layer appears darker compared with the Ge substrate, which suggests that diffraction contrast is also present. Diffraction contrast

**Table 1.** Film thickness of as-deposited and annealed (275 °C and 475 °C) poly- and epi-Fe films measured from BFTEM images. Samples were tilted to edge-on condition. The numbers in brackets show the percentage increase in the thickness of the film after nitrogen anneal.

| Temperature (°C) | Thickness (nm)                                |   |
|------------------|---|---|
|                  | Poly- Fe film<br>(% increase<br>in thickness) | Epi-Fe film<br>(% increase<br>in thickness) |
| As-deposited     | 30  | 22.5  |
| 275              | 36 [20%]                                      | 25.5 [ca. 13%]                              |
| 475              | 60 [100%]                                     | 44 [ca. 96%]                                |

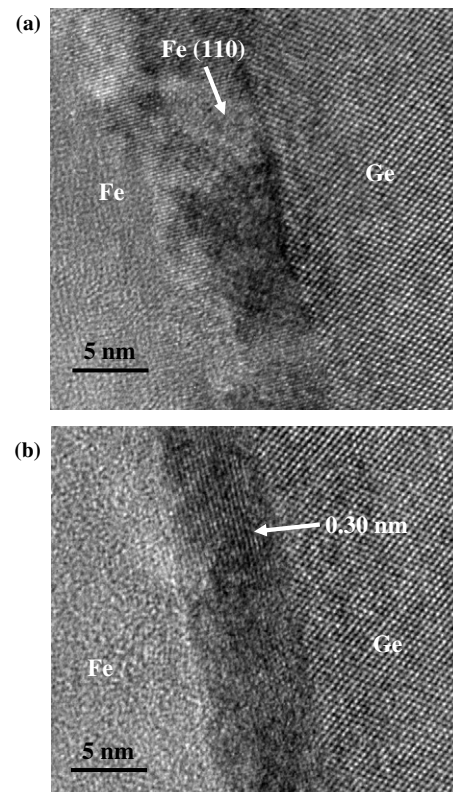


**Figure 2.** HRTEM images of (a) and (b) different regions of the interface of epi-Fe RTA 275 °C.

can be attributed to the presence of another phase (with a different crystallographic orientation) which scatters electron differently, in this case more strongly, compared with the epi-Fe film and Ge substrate. A different region in the same sample with similar dark contrast shows lattice fringes (figure 2(b)) with interplanar spacing ca 0.30 nm, which may be attributed to Fe<sub>3</sub>Ge  $\langle 101 \rangle$  planes. Several attempts were made to tilt the crystal to its zone axis to determine its crystal structure, but they were severely limited by the thickness of this layer. However, STEM-EDX analyses performed on various regions along this dark band yield Fe : Ge (in at%) of  $\sim 3 : 1$ .

Field-dependent magnetization ( $M-H$ ) loops are used to study the magnetic property of the as-deposited and annealed films. The in-plane  $M-H$  loops of the poly-Fe films (as-deposited and annealed) are presented in figure 3(a). The as-deposited poly-Fe film exhibits an almost rectangular  $M-H$

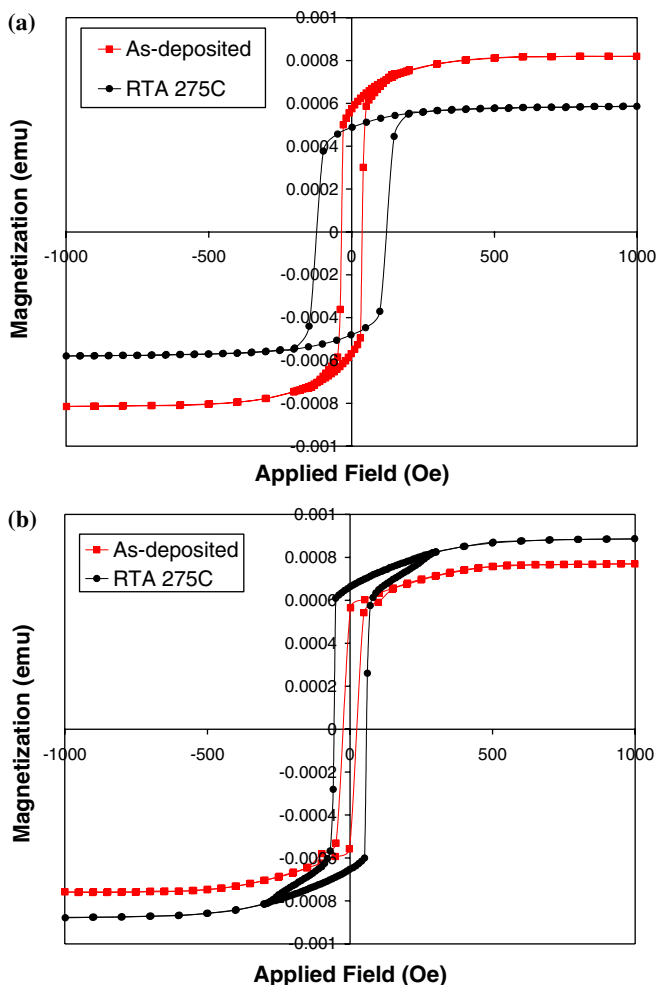


**Figure 3.**  $M$ - $H$  loops of as-deposited and annealed (275 °C) (a) poly-Fe films and (b) epi-Fe films.

loop with squareness and coercivity of 0.7 and 37.2 Oe. After a 275 °C anneal, the saturation magnetization decreased to 0.7 of the original value and the coercivity increased by a factor of 3.2. The  $M$ - $H$  loops of the as-deposited and annealed epi-Fe films exhibit similar squareness (figure 3(b)). The coercivity of the as-deposited epi-Fe film is 23.9 Oe, much lower than the as-deposited poly-Fe film, analogous to that reported by Lou *et al* [10]. The saturation magnetization increased by a factor of 1.2 upon annealing at 275 °C is observed. Several samples have been analyzed to confirm reproducibility. Our results are different from previous reports that suggest intermixing forms magnetically dead Fe-Ge layers [8, 11]. If epi-Fe is the only ferromagnetic phase present before and after the nitrogen anneal at 275 °C, the saturation magnetization will decrease with the thickness of epi-Fe consumed, analogous to the poly-Fe film. An increase in magnetization would

suggest that the germanide layer is ferromagnetic. There is no literature work on ferromagnetism of Fe-rich germanides. In addition, although Moya *et al* have reported magnetism in Finemet (FeSiB-based alloy), they did not report any VSM results so it is impossible to make any direct comparisons with the magnetization [12]. At this stage, we cannot say with absolute confidence that the Fe<sub>3</sub>Ge phase is solely responsible for the enhanced saturation magnetization, but while that is a possibility, other Fe-rich phases can also contribute to the enhanced magnetization. The increased coercivity in both poly-Fe and epi-Fe films can be attributed to an increase in the number of defects (such as grain boundaries) in the annealed film. No  $M$ - $H$  loops are observed at 475 °C for both poly- and epi- Fe films (not presented here).

#### 4. Conclusion

In conclusion, we have demonstrated a method for the formation of Fe-rich germanide in epi-Fe/Ge (001) by magnetron sputtering and nitrogen anneal and have also established the enhanced ferromagnetic nature of this Fe-rich germanide layer by  $M$ - $H$  loops analysis. We also made a comparison with poly-Fe films and observed a decrease in the saturation magnetization of these films. The behaviour of the epi-Fe films is surprising and we attribute it to the presence of Fe<sub>3</sub>Ge in the annealed epi-Fe films. We have also observed less intermixing in the epi-Fe film/Ge system than in the poly-Fe film/Ge system.

#### References

- [1] Wolf S A, Awschalom D D, Buhrman R A, Daughton J M, von Molnar S, Roukes M L, Chtchkanova A Y and Tregler D M 2001 *Science* **294** 1488
- [2] Roy W V, Dorpe P V, Vanheertum R, Vandormael P-J and Borghs G 2007 *IEEE Trans. Electron. Devices* **54** 933
- [3] Schloemann E, Tustison R, Weissman J, Van Hook H J and Varitimos T 1998 *J. Appl. Phys.* **63** 3410
- [4] Prinz G A and Krebs J J 1981 *Appl. Phys. Lett.* **39** 397
- [5] Kneeler E M, Jonker B T, Thibado P M, Wagner R J, Shanabrook B V and Whitman L J 1997 *Phys. Rev. B* **56** 8163
- [6] Florczak J M and Dan Ahlberg E 1991 *Phys. Rev. B* **44** 9338
- [7] Filipe A, Schuhl A and Galtier P 1997 *Appl. Phys. Lett.* **70** 129
- [8] Ma P and Norton P R 1997 *Phys. Rev. B* **56** 9881
- [9] Taria S, Sporken R, Aoki T, Smith D J, Metlushko V, Abuel-Rub K and Sivnanathan S 2002 *J. Vac. Sci. Technol. B* **20** 1856
- [10] Lou J, Daigle A, Chen L, Wu Y Q, Harris V G, Vittoria C and Sun N X 2006 *Appl. Phys. Lett.* **89** 112501
- [11] Heinrich B and Bland J A C (ed) 1994 *Ultrathin Magnetic Structures II* vol 2 (Berlin: Springer) p 35
- [12] Moya J A, Cremaschi V J and Sirkin H 2007 *Physica B* **389** 159